# Title: The role of snow cover on ice regime across Songhua River Basin, Northeast China

Qian Yang[1, 2], Kaishan Song[1, *], Xiaohua Hao[3], Zhidan Wen[2], Yue Tan[1], and Weibang Li[1]

[1]Jilin Jianzhu University, Xincheng Road 5088, Changchun 130118 China; E-Mail: jluyangqian10@hotmail.com

[2] Northeast Institute of Geography and Agroecology, Chinese Academy of Sciences, Shengbei Street 4888, Changchun 130102 China; E-Mail: songks@neigae.ac.cn;

[3] Northwest Institute of Eco-Environment and Resources, Chinese Academy of Sciences, Donggang West Road 322, Lanzhou 730000, China; E-Mail: haoxh@lzb.ac.cn;

*Correspondence to*: Song K. S. (songks@neigae.ac.cn)

**Abstract:** The Songhua River Basin, located in Northeast China, is an area sensitive to global warming that could be impacted by changes in lake and river ice regimes. The regional role and trends of lake and river ice of this area have been scarcely investigated and are critical for aquatic ecosystems, climate variability, and human activities. Using ice records of local hydrological stations, we examined the spatial variations of the ice phenology and ice thickness in the Songhua River Basin from 2010 to 2015 and explored the role of snow depth and air temperature on ice regime. All of five river ice phenology indicators, including freeze-up start, freeze-up end, break-up start, break-up end and complete frozen duration, showed a latitudinal distribution and a changing direction from southeast to northwest. Five typical geographic zones were identified applying a rotated empirical orthogonal function. Maximum ice thickness had a higher correlation with ice phenology, especially with the break-up process. Six Bayesian regression models were built between ice thickness, air temperature, and snow depth in three sub-basins of the Songhua River Basin. Results showed significant and positive correlations between snow cover and ice thickness when freshwater was completely frozen. Rather than by air temperature, ice thickness was influenced by negative cumulative air temperature through the heat loss of ice formation and decay.

**Keywords.** River ice, ice phenology, ice thickness, snow on ice, air temperature, rotated empirical orthogonal function

## 1 Introduction

The freeze-thaw process of surface ice of temperate lakes and rivers plays a crucial role in the interactions among the climate system(Yang et al., 2020), freshwater ecosystems (Kwok and Fahnestock, 1996) and the biological environment (Prowse and Beltaos, 2002). The presence of freshwater ice is closely associated with social and economic activities, ranging from human-made structures, water transportation, to winter recreation (Williams and Stefan, 2006;Lindenschmidt et al., 2017). Ice cover on rivers and lakes exerts large forces due to thermal expansion and could cause extensive infrastructure losses to bridges, docks, and shorelines (Shuter et al., 2012). Ice cover on waterbodies also provides a natural barrier between the atmosphere and water. Ice cover also blocks the solar radiation necessary for photosynthesis to provide

enough dissolved oxygen for fish, thus can have a negative effect on freshwater ecosystems and, in extreme cases, lead to winter kill of fish (Hampton et al., 2017). Generally, the duration of freshwater ice has shown a declining trend, with later freeze-up and earlier break-up throughout the northern hemisphere. For example, freeze-up has been occurring 0.57 days per decade later and break-up 0.63 days per decade earlier during the periods of 1846-1995 (Magnuson et al., 2000;Sharma et al., 2019;Beltaos and Prowse, 2009). To evaluate the influence of ice regimes on the regional climate and human environment, and provide helpful information for regional projections of climate and ice-river floods, a robust and quantitative analysis on ice processes is necessary. Despite the growing importance of river ice under global warming, very little work has been undertaken to explain the considerable variation of ice characteristics in Northeast China, where lakes and rivers are frozen for as long as five to six months a year.

The earliest ice record in the literature dates back to 150 years ago (Magnuson et al., 2000). Ice development and ice diversity scales have been regarded as sensitive climate indicators. Ice phenology and ice thickness have been studied to gain a deeper understanding of ice processes. At medium and large scales, optical remote sensing data are widely used for deriving ice phenology (Song et al., 2014;Šmejkalová et al., 2016), while microwave remote sensing are used to estimate ice thickness and snow depth over ice (Zhang et al., 2019;Kang et al., 2014). Wide-range satellites make it possible to link ice characteristic with climate indices, such as air temperature (Yang et al., 2020) or large-scale teleconnections (Ionita et al., 2018), but their spatial resolutions are too large to detect ice thickness and snow depth accurately at small scales. For example, the microwave satellite data of AMSR-E have a spatial resolution of 25 km, but the largest width of Nenjiang River only ranges from 170 to 180 meters. The spatial resolution limits the application of satellite observations to precisely inverse ice thickness, let alone snow depth.

In terms of point-based measurements, the most commonly used ground observations include regular observations, ice charts, volunteer monitoring and field measurements (Duguay et al., 2015). Ground observations depend on spatial distribution and representation, and are limited by the accessibility of surface-based networks and the range of field measurement. Ice parameters differ greatly from point to point on a given river (Pavelsky and Smith, 2004), and the uneven distribution of hydrological stations poses an obstacle to gaining a comprehensive understanding of river ice. Various models have been implemented to derive ice phenology and ice thickness, such as physically-based models (Park et al., 2016), linear regressions (Palecki and Barry, 1986;Williams and Stefan, 2006), logistic regressions (Yang et al., 2020) and artificial neural networks (Seidou et al., 2006;Zaier et al., 2010). These models consider the energy exchange and physical changes of freshwater ice and require detailed information and data support, including hydrological, meteorological, hydraulic and morphological information. Fixed stations are normally located around the river mouth of certain rivers, so these models are limited by the input data available (Pavelsky and Smith, 2004). Both modelling and remote sensing monitoring require sufficient historical ice records to validate and improve accuracy and reliability.

The ice cover of water bodies experiences three stages during which ice phenology, ice thickness and ice composition change greatly. These stages are: freeze-up, ice growth, and break-up (Duguay et al., 2015).

Although air temperature greatly influences the freeze-thaw cycle of river ice, the effect of snow cover can't be ignored. Generally, snow depth outweighs air temperature during the ice forming process and increasing snow depth provides favourable conditions for thicker ice (Morris et al., 2005;Park et al., 2016). Compared to other studies, air temperature had a greater effect on ice thickness than snow depth and were attributed this to the high snowfall in the study area (Gao and Stefan, 2004). Besides, in situ observations at Russian river mouths where ice thickness decreased had not shown any significant correlation between ice thickness and snow depth (Shiklomanov and Lammers, 2014). Those studies analysed the relationship in view of spatial distributions and ignored the changing status of ice formation processes. The relative influence of snow depth and air temperature on the ice regime deserves further exploration in Northeast China.

The surface-based networks, including climatic and hydrological stations, have been established for tracing climate and hydrological changes in Northeast China, which are limited by the accessibility of surface-based networks and the range of filed measurement. To evaluate the influence of ice regime on regional climate and human environment, a robust investigation and quantitative analysis on ice regime is necessary, which provide helpful information for projecting future changes in the ice regime. The previous work explored the ice process in at one or more locations on a given river and ignored the changing regional pattern of ice development due to sparse location. The objectives of this study are to: (1) investigate and compare the spatial distribution of ice phenology and thickness in Northeast China; (2) quantitatively explore the influence of snow cover and air temperature on ice regime.

## 2 Materials and methods

### 2.1 Study area

The Songhua River Basin is located in the middle of Northeast China (Figure 1), and includes Jilin Province, Heilongjiang Province, and the eastern part of Inner Mongolia Autonomous Region. The Songhua River is the third-longest river in China, and has three main tributaries: Nenjiang River, Main Songhua River, and Second Songhua River (Zhao et al., 2018;Khan et al., 2018). The basins of the three tributary rivers include: Nenjiang Basin (NJ), the Downstream Songhua River Basin (SD), and the Upstream Songhua River Basin (SU) (Figure 1). The Nenjiang River has a length of 1370 km, and the corresponding drainage has an area of $2.55 \times 10^6$ thousand $km^2$; the Main Songhua River has a length of 939 km and the downstream catchment of the Songhua River Basin (SD) has an area of $1.86 \times 10^6$ $km^2$; the Second Songhua River has a length of 958 km and the upstream catchment of the Songhua River Basin (SU) has an area of $6.19 \times 10^6$ $km^2$ (Yang et al., 2018;Chen et al., 2019). The whole Songhua River Basin is characterized by temperate and cold temperate climates: winter is long and cold; spring is windy and dry. Annual average air temperature ranges between 3 to 5℃, while annual precipitation ranges from 400 to 800 cm from the southeast to the northwest. (Wang et al., 2015;Wang et al., 2018).

[Figure 1 is added here]

### 2.2 Data Source

#### 2.2.1 Ice phenology

The hydrographic bureau of the Chinese Ministry of Water Resources has established a remarkable observation network for ice regimes. The ice records of the Songhua River Basin were obtained from the annual hydrological report, including ice phenology, ice thickness, snow depth on ice and air temperature on bank (BAT) (Annual hydrological report, 2010-2015). To analyse the spatial pattern of the ice regime, we explored five river ice parameters with the corresponding day of year (DOY) from 158 stations. We located 50, 36 and 72 stations in the NJ, SU and SD basins, respectively. For each record, five lake ice phenological events were derived from the annual hydrological report; the definitions referred to specification for observation of ice regimes in rivers and previous works (Cai et al., 2019;Yang et al., 2019;Duguay et al., 2015) :

- Freeze-up start (FUS) is considered the first day when floating ice can be observed with temperatures below 0 ℃;
- Freeze-up end (FUE) is the day when a steady ice carapace can be observed on the river, and the area of ice cover is more than 80% in the view range;
- Break-up start (BUS) is the first day when ice melting can be observed with surface ponding;
- Break-up end (BUE) is the day when the surface is mainly covered by open water and the area of open water exceed 20%;
- Complete frozen duration (CFD) is the ice cover duration when the lake is completely frozen during the winter, from FUE to BUS.

#### 2.2.2 Ice thickness

To study seasonal changes in ice thickness (IT) and establish the regression model, we used ice thickness, snow depth and air temperature from 120 stations for the period ranging from 2010 to 2015. We used 37, 28 and 55 stations located in the NJ, SU and SD basins, respectively. The hydrological report provided ice thickness, snow depth on ice and BAT every five days from November through April, totalling 37 measurements in one cold season. The yearly maximum ice thickness (MIT) of the river centre and the corresponding DOY were calculated from five-day records. The average snow depth (ASD) was calculated from the mean of three or four measurements around the ice hole for ice thickness measurement without human disturbance. To enhance the performance of the regression model, negative cumulative air temperature was calculated from air temperature from November to March.

### 2.3 Data analysis

2.3.1 Kriging

Kriging has been widely used to spatially interpolate in situ measurements of ice phenology to understand its spatial distribution (Choiński et al., 2015;Jenson et al., 2007). Kriging assumes a correlation between regionalized variables and variograms that reflects randomization and structuredness of regionalized variables. It estimates unknown values based on the best linear unbiased estimator with minimal variance, expressed as:

$$\hat{Z}(s_o) = \sum_{i=1}^{N} \lambda_i Z(s_i)$$

where $\hat{Z}(s_o)$ is the estimate by kriging at an unknown point $s_o$, $Z(s_i)$ is the variable at a measured point $s_i$, N is the number of measured points. $\lambda_i$ is a weight for $Z(s_i)$, and relies on the spatial arrangement of the measured values and the distance between the prediction location and the measured location (C.R. Paramasivam, 2019). The average values of five ice phenology indicators during the six years were interpolated to create isophenes, i.e., contour lines connecting locations with the same ice phenology.

2.3.2 Rotated empirical orthogonal function (REOF)

Empirical orthogonal function (EOF) decomposition is commonly used in climate and hydrological analyses (Bian et al., 2019;Yang et al., 2017). Its basic principle is to decompose the field containing *p* spatial points (variable) over time. If the sample size is *n*, then the data value $x_{ij}$ including specific spatial point *i* and specific time *j* in the field can be regarded as the linear combination of spatial modes and temporal modes according to equation:

$$S_{b^2}^2 = \frac{1}{mM} \sum_{j=1}^{M} \sum_{p=1}^{m} (b_{jp}^2 - \overline{b^2})^2$$

where $b_{jp}$ is the *j th* loading coefficient of the *p th* EOF mode.

The major advantages of the EOF method is to separate the uncorrelated components that confuse the spatial information and make it hard to interpret a physical phenomenon. In order to solve these problems, a rotated EOF (REOF) rotates the original EOF matrix into a new matrix in which the squared elements of the eigenvectors are maximum, which can better reflect changes across different geographic regions and identify correlations. This paper presented the first four load vectors of the CFD decomposed by REOF and their corresponding principal components (PC) to identify the typical geographic zones in Northeast China.

2.3.3 Bayesian linear regression

Ice thickness had been modelled by air temperature and snow depth using Bayesian linear regression (BLR), which has been widely used in hydrological and environmental analyses (Zhao et al., 2013;Gao et al., 2014). BLR treats regression coefficients and the disturbance variance as random variables, rather than fixed but unknown quantities. This assumption leads to a more flexible model and intuitive inferences (Barber, 2008). The BLR model was implemented through two models: a prior probability model considered the probability distribution of the regression coefficients and the disturbance; a posterior model predicted the response using the prior probability mentioned below. The performance of the regression model was evaluated using the determination coefficient $R^2$ and the root mean square error (RMSE). In this paper, the Y data were the five-day ice thickness values, and the X data included snow depth over ice and air temperature on the river bank. The calculation of the regression used the in-situ measurements from November to March and excluded the ice records of April due to unsteady ice conditions. Two types of air temperature were considered: BAT and negative cumulative air temperature (ATC). Additionally, the Pearson correlation was calculated to analyse the relationship among the five ice phenology events and ice-related parameters, including MIT, ASD, and BAT(Gao and Stefan, 1999;Williams et al., 2004).

## 3 Results and discussion

### 3.1 Spatial variations of river ice phenology

#### 3.1.1 Freeze-up and break-up process

Figure 2 illustrates the average spatial distribution of FUS and FUE interpolated by kriging and the isophenes in the Songhua River Basin of Northeast China from 2010 to 2015. Figure 3 illustrates the spatial distribution of the BUS and BUE. The corresponding statistics are listed in Table 1. FUS ranged from October 28$^{th}$ to November 21$^{st}$ with a mean value of November 7$^{th}$, and FUE ranged from November 7$^{th}$ to December 8$^{th}$ with a mean value of November 22$^{nd}$. BUS ranged from March 24$^{th}$ to April 20$^{th}$ with a mean value of April 9$^{th}$, and BUE ranged from March 31$^{th}$ to April 27$^{th}$ with a mean value of April 15$^{th}$. These four parameters showed a latitudinal gradient: FUS and FUE decreased while BUS and BUE increased as the latitude increased, except in NJ. The middle part of NJ had the highest FUS and FUE and decreased to the southern and northern part. As the latitude decreased, the air temperature tended to increase, leading to later freeze-up and earlier break-up with shorter ice-covered duration; vice versa.

[Figure 2 is added here]

[Figure 3 is added here]

[Table 1 is added here]

#### 3.1.2 Complete frozen duration

Figure 4(a) illustrates the average spatial distribution of CFD interpolated by kriging and the isophenes in the Songhua River Basin from 2010 to 2015. CFD ranged from 110.74 to 163.00 days with a mean value of 137.86 days, increasing with latitude. Interestingly, the isophenes of CFD had different directionality, increasing from the southeast to northwest, which could also be found in the other four ice phenologists. Both FUS and FUE correlated negatively with latitude, with coefficients of -0.66 and -0.53, respectively ($n=158$, $p < 0.001$). BUS, BUE and CFD were all positively correlated with latitude with coefficients of 0.48, 0.57 and 0.55, respectively ($n=158$, $p < 0.001$). High values indicated a delay in the ice phenology event. The general spatial trend was a tendency to advance as the latitude increased for the FUS and FUE, a tendency for delay for BUS and BUE, and a lengthening tendency for CFD. A decreasing solar radiation with latitude could explain this trend, which is directly connected with the ice thaw and melting processes.

To find the spatial distribution of ice durations, average values of CFD between 2010 and 2015 were decomposed by REOF, and the spatial distribution of the first four PC are shown in Figures 4 (c)-(f) interpolated by kriging. The first to fourth PC modes accounted for 45.89%, 13.22%, 12.62%, and 12.00%, respectively, with the cumulative variance of 83.73%. The PC data ranged from -0.22 to 0.15, and the areas with high values presented a planar distribution, which were further regarded as five typical geographic zones considering the topography of Northeast China. Zone 1, located in the Three River Plain, where Heilongjiang, Wusuli, and Songhua River converge together, was identified from the first PC. Zone 2, located around

Heaven Lake of Changbai Mountain, in the southernmost part and which has the highest elevation of 2565 m, was identified from the second PC mode. We excluded a planar distribution above Zone 2 because of the gentle terrain in the Songhua River Basin. The middle part of the Songhua River Basin accounts for a large area where no typical zones were found. The REOF was good at enhancing the high-value areas, and the PC data of this area around 0 were ignored. Zone 3, located on the eastern edge of the three basins with relatively high elevation along the ridge of Changbai Mountain, was identified from the third PC mode. Based on the fourth PC mode, Zone 4 was determined in the northernmost part along the ridge of Xiao Higgan Mountain where it meets with Da Higgan Mountain. Zone 5 almost covered the southern part of the NJ basin along the ridge of Da Higgan Mountain and appeared in the second, third, and fourth PC. The final distribution was identified from the convergence area of these three modes.

[Figure 4 is added here]

### 3.2 Variations of ice thickness

#### 3.2.1 Spatial pattern of ice thickness

Figure 5 illustrates the spatial distribution of the yearly maximum ice thickness (MIT) of the river centre and the corresponding DOY. Table 2 summarized the statistical result of MIT and DOY. MIT ranged from 12 cm to 146 cm, with an average value of 78 cm. The MIT between 76 and 100 cm accounted for the largest percentage of 43.33%, followed by 31.67% of MIT between 50 and 75 cm. Five stations had MIT greater than 125 cm. Two stations were located in Zone 3 and three stations in Zone 4. The DOY of MIT had an average value of February 21$^{st}$, and MIT mainly occurred 59 and 40 times in February and March, respectively. Four of the five highest MITs greater than 125 cm happened in March, which is consistent with the inter-annual changes in ice development shown in Figure 6. The results suggested that the river ice is always thickest and most steady in February or March, which is the best suitable time for human activities such as ice fishing and entertainment. The ice thickness didn't show the same latitudinal distribution as ice phenology, which suggested that more climate factor should be taken in to consideration, such as snow depth and wind.

[Figure 5 is added here]

[Table 2 is added here]

#### 3.2.2 Seasonal changes of ice thickness

Figure 6 displays the seasonal changes of ice development using ice thickness, average snow depth on ice, and BAT every five days from 2010 to 2015. Among the three basins, NJ had the highest snow depth of -29.15 ± 9.99℃, followed by -25.61 ± 9.02 ℃ in the SD, and -22.17 ± 7.33 cm in the SU. SD had the highest snow depth of 9.18 cm ± 3.39 cm on average level, followed by 8.35 cm ± 4.60 cm in SU, and 8.23cm ± 3.92 cm in NJ. The changes in IT and ASD had similar overall trend, while BAT followed the opposite trend. Both IT and ASD increased from November and reached the peak in March, then dropped at the beginning of April. The ASD showed an obvious trend and reached the bottom in the middle of January, which is earlier than the

peaks of MIT and ASD. The NJ and the SD basins underwent greater fluctuations than the SU basin, because river ice may freeze and thaw alternatively at relatively low temperatures. The changes of ice characteristics differed greatly due to time and location; an analysis of the annual changes was not conducted because the time series were not long enough.

[Figure 6 is added here]

### 3.3 The relationship between ice regime and climate factors

#### 3.3.1 Correlation analysis

Figure 7 displays the correlation matrix between lake ice phenology events and three parameters, covering yearly average values of ASD, BAT, and MIT with a dataset size of 120 stations. Colour intensity and sizes of the ellipses are proportional to the correlation coefficients. MIT had a higher correlation with four of the five indices than ASD and BAT, except with FUS, with which both MIT and BUE had the highest correlation of 0.63 ($p<0.01$, $n=120$). During the freeze-up process, two freeze-up dates had a negative correlation with MIT and ASD; during the break-up, two break-up dates had a positive correlation with MIT and ASD. CFD had a positive correlation with MIT and ASD. The situation of BAT was contrary to that of MIT and ASD. Regarding to the annual changes, no significant correlation was found between snow depth and five ice phenology events in Figure 7.

[Figure 7 is added here]

Figure 8 shows the bivariate scatter plots between yearly maximum ice thickness (MIT) and five ice phenology indicators with regression equations. The break-up process had a negative correlation with MIT, while freeze-up had a positive correlation. Besides, the break-up process had a higher correlation with MIT, and BUS had the highest correlation coefficients with MIT of 0.65 ($p<0.01$). CFD also had a positive correlation with MIT of 0.55 ($P<0.01$), which means that a thicker ice cover in winter leads to a delay in melting time in spring. The break-up not only depends on the spring climate conditions, but is also influenced by ice thickness during last winter. A thicker ice cover stores more heat in winter, taking a longer time to melt in spring. The limited performance of the regression model could be attributed to the difficulties in determining river ice phenology. Although a uniform observation protocol was required, the repaid transition between frozen river and open water for two or three days with floating ice and the inhomogeneities among different stations could not be ignored.

[Figure 8 is added here]

To further explore the role of snow cover, the monthly correlation coefficients between IT and ASD, and IT and BAT were calculated and listed in Table 3. The correlation coefficients between IT and ASD increased from November to March and reached a peak of 0.75 in March when ice was thickest. This indicated an increasingly important role of snow depth on ice thickness as the ice accumulated. The higher correlation coefficients between IT and BAT in November and December revealed that BAT played a more important

role in the freeze-up process. Moreover, whether the status of river ice was steady or not also could not be neglected when studying the role of snow cover.

The positive correlation coefficient between snow depth and ice thickness (Table 3) revealed two opposite effects of snow depth during ice development: during the ice-growth process, snow depth protects the ice from cold air and slows down the growth rate of ice thickness; during the ice-decay process, the lake bottom ice stops to grow, and the snow mixes with surface ice into slush and promotes melting.

[Table 3 is added here]

### 3.3.2 Regression modelling

Figure 9 illustrates the scatter plot between measured and predicted ice thickness using Bayesian linear regression in three sub-basins in Northeast China. $R^2$ ranged from 0.81 to 0.95, and RMSE ranged from 0.08 to 0.17. The model worked best in the SU basin, followed by the NJ and the SD basins. Figure 9 indicates that snow depth outweighed air temperature in terms of effect on ice thickness, which is consistent with previous studies. Moreover, replacing BAT with ATC enhanced the model performance in all three basins, revealing a more important role of ATC than BAT.

[Figure 9 is added here]

The correlation between air temperature and ice regime was not as significant as in previous studies for several reasons. Average air temperatures were most commonly calculated over fixed time periods at regional scales, for example as moving averages for certain time periods. The seasonal changes of air temperature were ignored, as well as their effects within one cold season. The negative ATC behaved better than BAT when building the Bayesian regression equation, which suggested that heat exchanges between river surface and atmosphere dominated the ice process. Heat loss is mainly made up of sensible and latent heat exchange, which is proportional to negative ATC during the cooling process. During the complete frozen duration, snow depth along with wind speed began to influence the heat exchange and ice thickening. Air temperature exerted a lesser effect on spring break-up, which is more dependent on the ice thickness and snow depth. In summary, snow depth dominated the ice process when the river was completely frozen, while cumulative air temperature dominated during the transition process.

## 4 Conclusions

Five river ice phenology indicators, including FUE, FUS, BUE, BUS, and CFD, in the Songhua River Basin of Northeast China have been investigated using in situ measurements for the period 2010 to 2015 using kriging and REOF methods. The FUS and FUE decreased while the BUS, BUE, and CFD increased with latitude. The five river ice phenology indicators followed the latitudinal gradient and a changing direction from southeast to northwest. The highest MIT over 125 cm were distributed along the ridge of Da Hagan Lin and Changbai Mountain, and MIT occurred most often in February and March, which indicated that this is the safest period for human activities such as navigation and winter recreation. Five typical geographic zones were identified from the first four PC modes of CFD, covering Changbai Mountain, Three River Plain, Da

Higgan Mountain, and Xiao Higgan Mountain, providing a deeper understanding of river ice distribution and its relationship with geographic locations and topography in Northeast China.

Within one cold season, ice thickness and snow depth showed similar seasonal changes, i.e. first increased and then decreased, while air temperature showed an opposite trend. The peaks of snow depth and ice thickness fell behind air temperature for almost one month. High correlation coefficients between yearly maximum ice thickness and ice phenology indicators revealed that ice phenology is closely related to ice thickness, especially in the break-up process. The yearly analysis failed to explain the relationship between ice regime and snow depth and air temperature. Based on monthly correlation analysis, snow cover played an increasingly important role as the ice cover become steady. Additionally, air temperature associated with ice phenology more closely than ice thickness.

Six Bayesian regression models were built between ice thickness and air temperature and snow depth in three sub-basins of Songhua River, considering two types of air temperature: air temperature on bank and negative cumulative air temperature. Results showed that snow cover correlated with ice thickness significantly and positively during the periods when the freshwater was completely frozen, and negative cumulative air temperature influenced the thickness rather than air temperature through the heat loss of ice formation and decay. The negative ATC behaved better than BAT when building the Bayesian regression equation, which suggested that heat exchanges between the river surface and the atmosphere dominated the ice process.

This study aimed at exploring the regional patterns of river ice development based on in situ measurements and was limited by data accessibility. Remote sensing data could provide long-term and wide-range information for ice thickness and ice phenology since 1980, expanding our study scope. The work herein will provide a valuable reference for the retrieval of ice development by remote sensing. Knowing the long-term change of river ice and the future projection could provide information for evaluating the influence of climate on social-economics, ecological environment and human activists across the riparian zones.

**Abbreviations**

The following abbreviations are used in this manuscript:

AMSR-E Advanced Microwave Scanning Radiometer- Earth Observing System
ASD Average Snow depth
ATC Cumulative air temperature
BAT Air temperature on bank
BLR Bayesian linear regression
BUS Break-up start
BUE Break-up end
CFD Completely frozen duration
DOY Day of year
EOF Empirical orthogonal function

FUS Freeze-up start

FUE Freeze-up end

IP Ice phenology

IT Ice thickness

NJ Nenjiang River Basin

MIT Maximum ice thickness

PC Principal component

REOF Rotated empirical orthogonal function

RMSE Root mean square error

SD Downstream Songhua River Basin

SRTM Shuttle Radar Topography Mission

SU Upstream Songhua River Basin

## Author Contribution

Song K.S. and Yang Q. designed and conducted the idea of this study. Yang Q. Wen Z.D. wrote the paper and analysed the data cooperatively; Hao X.H. provided value suggestion for the structure of study and paper; Li W.B. and Tan Y. exerted efforts on data processing and graphing. This article is a result of collaboration with all listed co-authors.

## Competing interest

The authors reported no potential conflict of interest.


## Acknowledgments

The research was sponsored by the National Natural Science Foundation of China (41801283, 41971325, 41730104). The anonymous reviewers to improve the quality of this manuscript are greatly appreciated.


## References


Barber, J. J.: Bayesian Core: A Practical Approach to Computational Bayesian Statistics, Journal of the American Statistical Association, 103, 432-433, 2008.

Beltaos, S., and Prowse, T.: River-ice hydrology in a shrinking cryosphere, 23, 122-144, https://doi.org/10.1002/hyp.7165, 2009.

Bian, Y., Yue, J., Gao, W., Li, Z., Lu, D., Xiang, Y., and Chen, J.: Analysis of the Spatiotemporal Changes of Ice Sheet Mass and Driving Factors in Greenland, Remote Sensing, 11, https://doi.org/10.3390/rs11070862, 2019.

C.R. Paramasivam, S. V.: An Introduction to Various Spatial Analysis Techniques, in: GIS and Geostatistical Techniques for Groundwater Science, edited by: Senapathi Venkatramanan, M. V. P., Sang Yong Chung, Elsevier, 23-30, 2019.

Cai, Y., Ke, C.-Q., Yao, G., and Shen, X.: MODIS-observed variations of lake ice

phenology in Xinjiang, China, Climatic Change, https://doi.org/10.1007/s10584-019-02623-2, 2019.
Chen, H., Zhang, W., Nie, N., and Guo, Y.: Long-term groundwater storage variations estimated in the Songhua River Basin by using GRACE products, land surface models, and in-situ observations, Sci Total Environ, 649, 372-387, https://doi.org/10.1016/j.scitotenv.2018.08.352, 2019.
Choiński, A., Ptak, M., Skowron, R., and Strzelczak, A.: Changes in ice phenology on polish lakes from 1961 to 2010 related to location and morphometry, Limnologica, 53, 42-49, 2015.
Duguay, C. R., Bernier, M., Gauthier, Y., and Kouraev, A.: Remote sensing of lake and river ice, 273-306 pp., 2015.
Gao, B. S., and Stefan, H. G.: Multiple linear regression for lake ice and lake temperature characterisitcs, Journal of Cold Regions Engineering, 13, 59-77, 1999.
Gao, S., and Stefan, H. G.: Potential Climate Change Effects on Ice Covers of Five Freshwater Lakes, Journal of Hydrologic Engineering, 9, 226-234, https://doi.org/doi:10.1061/(ASCE)1084-0699(2004)9:3(226), 2004.
Gao, S., Zhu, Z., Liu, S., Jin, R., Yang, G., Tan, L. J. I. J. o. A. E. O., and Geoinformation: Estimating the spatial distribution of soil moisture based on Bayesian maximum entropy method with auxiliary data from remote sensing, 32, 54-66, 2014.
Hampton, S. E., Galloway, A. W., Powers, S. M., Ozersky, T., Woo, K. H., Batt, R. D., Labou, S. G., O'Reilly, C. M., Sharma, S., Lottig, N. R., Stanley, E. H., North, R. L., Stockwell, J. D., Adrian, R., Weyhenmeyer, G. A., Arvola, L., Baulch, H. M., Bertani, I., Bowman, L. L., Jr., Carey, C. C., Catalan, J., Colom-Montero, W., Domine, L. M., Felip, M., Granados, I., Gries, C., Grossart, H. P., Haberman, J., Haldna, M., Hayden, B., Higgins, S. N., Jolley, J. C., Kahilainen, K. K., Kaup, E., Kehoe, M. J., MacIntyre, S., Mackay, A. W., Mariash, H. L., McKay, R. M., Nixdorf, B., Noges, P., Noges, T., Palmer, M., Pierson, D. C., Post, D. M., Pruett, M. J., Rautio, M., Read, J. S., Roberts, S. L., Rucker, J., Sadro, S., Silow, E. A., Smith, D. E., Sterner, R. W., Swann, G. E., Timofeyev, M. A., Toro, M., Twiss, M. R., Vogt, R. J., Watson, S. B., Whiteford, E. J., and Xenopoulos, M. A.: Ecology under lake ice, Ecol Lett, 20, 98-111, https://doi.org/10.1111/ele.12699, 2017.
Ionita, M., Badaluta, C. A., Scholz, P., and Chelcea, S.: Vanishing river ice cover in the lower part of the Danube basin - signs of a changing climate, Sci Rep, 8, 7948, https://doi.org/10.1038/s41598-018-26357-w, 2018.
Jenson, B. J., Magnuson, J. J., Card, V. M., Soranno, P. A., and Stewart, K. M.: Spatial Analysis of Ice Phenology Trends across the Laurentian Great Lakes Region during a Recent Warming Period, Limnology Oceanography, 52, 2013-2026, 2007.
Kang, K. K., Duguay, C. R., Lemmetyinen, J., and Gel, Y.: Estimation of ice thickness on large northern lakes from AMSR-E brightness temperature measurements, Remote Sensing of Environment, 150, 1-19, https://doi.org/10.1016/j.rse.2014.04.016, 2014.
Khan, M. I., Liu, D., Fu, Q., and Faiz, M. A.: Detecting the persistence of drying trends under changing climate conditions using four meteorological drought indices, Meteorological Applications, 25, 184-194, https://doi.org/10.1002/met.1680, 2018.
Kwok, R., and Fahnestock, M. A.: Ice Sheet Motion and Topography from Radar Interferometry, IEEE Transactions on Geoscience Remote Sensing, 34, 189-200, 1996.
Lindenschmidt, K.-E., Das, A., and Chu, T.: Air pockets and water lenses in the ice cover of the Slave River, Cold Regions Science and Technology, 136, 72-80, https://doi.org/10.1016/j.coldregions.2017.02.002, 2017.
Magnuson, J. J., Robertson, D. M., Benson, B. J., Wynne, R. H., Livingstone, D. M., Arai, T., Assel, R. A., Barry, R. G., Card, V., and Kuusisto, E.: Historical Trends in Lake and River Ice Cover in the Northern Hemisphere, Science, 289, 1743-1746, 2000.

Morris, K., Jeffries, M., and Duguay, C.: Model simulation of the effects of climate variability and change on lake ice in central Alaska, USA, in: Annals of Glaciology, Vol 40, 2005, edited by: MacAyeal, D. R., Annals of Glaciology-Series, 113-118, 2005.
Palecki, M. A., and Barry, R. G.: Freeze-up and Break-up of Lakes as an Index of Temperature Changes during the Transition Seasons: A Case Study for Finland, Journal of Applied Meteorology, 25:7, 893-902, 1986.
Park, H., Yoshikawa, Y., Oshima, K., Kim, Y., Ngo-Duc, T., Kimball, J. S., and Yang, D.: Quantification of Warming Climate-Induced Changes in Terrestrial Arctic River Ice Thickness and Phenology, Journal of Climate, 29, 1733-1754, https://doi.org/10.1175/jcli-d-15-0569.1, 2016.
Pavelsky, T. M., and Smith, L. C.: Spatial and temporal patterns in Arctic river ice breakup observed with MODIS and AVHRR time series, Remote Sensing of Environment, 93, 328-338, https://doi.org/10.1016/j.rse.2004.07.018, 2004.
Prowse, T. D., and Beltaos, S.: Climatic control of river-ice hydrology: a review, 16, 805-822, https://doi.org/10.1002/hyp.369, 2002.
Seidou, O., Ouarda, T. B. M. J., Bilodeau, L., Bruneau, B., and St-Hilaire, A.: Modeling ice growth on Canadian lakes using artificial neural networks, Water Resources Research, 42, 2526-2528, 2006.
Sharma, S., Blagrave, K., Magnuson, J. J., O'Reilly, C. M., Oliver, S., Batt, R. D., Magee, M. R., Straile, D., Weyhenmeyer, G. A., Winslow, L., and Woolway, R. I.: Widespread loss of lake ice around the Northern Hemisphere in a warming world, Nature Climate Change, 9, 227-231, https://doi.org/10.1038/s41558-018-0393-5, 2019.
Shiklomanov, A. I., and Lammers, R. B.: River ice responses to a warming Arctic—recent evidence from Russian rivers, Environmental Research Letters, 9, 035008, https://doi.org/10.1088/1748-9326/9/3/035008, 2014.
Shuter, B. J., Finstad, A. G., Helland, I. P., Zweimüller, I., and Hölker, F.: The role of winter phenology in shaping the ecology of freshwater fish and their sensitivities to climate change, Aquatic Sciences, 74, 637-657, 2012.
Šmejkalová, T., Edwards, M. E., and Dash, J.: Arctic lakes show strong decadal trend in earlier spring ice-out, Scientific Reports, 6, 38449, 2016.
Song, C., Huang, B., Ke, L., and Richards, K. S.: Remote sensing of alpine lake water environment changes on the Tibetan Plateau and surroundings: A review, Isprs Journal of Photogrammetry and Remote Sensing, 92, 26-37, https://doi.org/10.1016/j.isprsjprs.2014.03.001, 2014.
Wang, M., Lei, X., Liao, W., and Shang, Y.: Analysis of changes in flood regime using a distributed hydrological model: a case study in the Second Songhua River basin, China, International Journal of Water Resources Development, 34, 386-404, https://doi.org/10.1080/07900627.2018.1440538, 2018.
Wang, S., Wang, Y., Ran, L., and Su, T.: Climatic and anthropogenic impacts on runoff changes in the Songhua River basin over the last 56years (1955–2010), Northeastern China, Catena, 127, 258-269, https://doi.org/10.1016/j.catena.2015.01.004, 2015.
Williams, G., Layman, K. L., and Stefan, H. G.: Dependence of lake ice covers on climatic, geographic and bathymetric variables, Cold Regions Science Technology, 40, 145-164, 2004.
Williams, S. G., and Stefan, H. G.: Modeling of Lake Ice Characteristics in North America using Climate, Geography, and Lake Bathymetry, Journal of Cold Regions Engineering, 20, 140-167, 2006.
Yang, P., Xia, J., Zhan, C., Qiao, Y., and Wang, Y.: Monitoring the spatio-temporal changes of terrestrial water storage using GRACE data in the Tarim River basin between 2002 and 2015, Science of the Total Environment, 595, 218-228, 2017.

Yang, Q., Song, K., Hao, X., Chen, S., and Zhu, B.: An Assessment of Snow Cover Duration Variability Among Three Basins of Songhua River in Northeast China Using Binary Decision Tree, Chinese Geographical Science, 28, 946-956, https://doi.org/10.1007/s11769-018-1004-0, 2018.

Yang, Q., Song, K., Wen, Z., Hao, X., and Fang, C.: Recent trends of ice phenology for eight large lakes using MODIS products in Northeast China, International Journal of Remote Sensing, 40, 5388-5410, https://doi.org/10.1080/01431161.2019.1579939, 2019.

Yang, X., Pavelsky, T. M., and Allen, G. H.: The past and future of global river ice, Nature, 577, 69-73, https://doi.org/10.1038/s41586-019-1848-1, 2020.

Zaier, I., Shu, C., Ouarda, T. B. M. J., Seidou, O., and Chebana, F.: Estimation of ice thickness on lakes using artificial neural network ensembles, Journal of Hydrology, 383, 330-340, 2010.

Zhang, F., Li, Z., and Lindenschmidt, K.-E.: Potential of RADARSAT-2 to Improve Ice Thickness Calculations in Remote, Poorly Accessible Areas: A Case Study on the Slave River, Canada, Canadian Journal of Remote Sensing, 45, 234-245, https://doi.org/10.1080/07038992.2019.1567304, 2019.

Zhao, K., Valle, D., Popescu, S., Zhang, X., and Mallick, B.: Hyperspectral remote sensing of plant biochemistry using Bayesian model averaging with variable and band selection, Remote Sensing of Environment, 132, 102-119, https://doi.org/10.1016/j.rse.2012.12.026, 2013.

Zhao, Y., Song, K., Lv, L., Wen, Z., Du, J., and Shang, Y.: Relationship changes between CDOM and DOC in the Songhua River affected by highly polluted tributary, Northeast China, Environmental Science Pollution Research, 25, 25371-25382, 2018.

**Tables**

Table 1 Summary statistics of ice phenology interpolated by Kriging from 2010 to 2015. The ice phenology indicators included freeze-up start (FUS), freeze-up end (FUE), break-up start (BUS), break-up end (BUE), complete frozen duration (CFD). NJ, SD and SU represent the Nenjiang Basin, the downstream Songhua River Basin (SD) and the upstream Songhua River Basin (SU). DOY denotes day of year. Std Dev. denotes standard deviation.

| Basins | Statistics | FUS (DOY) | FUE (DOY) | BUS (DOY) | BUE (DOY) | CFD (day) |
|---|---|---|---|---|---|---|
| **NJ** | **Maximum** | 319.14 | 334.98 | 110.54 | 117.61 | 163.00 |
| | **Mean** | 307.02 | 324.58 | 98.65 | 106.64 | 139.39 |
| | **Minimum** | 301.41 | 311.30 | 84.53 | 90.40 | 119.11 |
| | **Std Dev.** | 3.91 | 5.69 | 8.16 | 6.80 | 13.22 |
| **SD** | **Maximum** | 321.08 | 334.36 | 110.01 | 102.84 | 154.06 |
| | **Mean** | 313.74 | 326.70 | 102.55 | 97.15 | 140.86 |
| | **Minimum** | 305.64 | 316.80 | 93.22 | 92.37 | 125.32 |
| | **Std Dev.** | 2.83 | 3.13 | 3.92 | 2.12 | 5.69 |
| **SU** | **Maximum** | 325.92 | 342.09 | 98.25 | 114.37 | 133.62 |
| | **Mean** | 320.39 | 334.35 | 91.93 | 106.43 | 122.61 |
| | **Minimum** | 313.79 | 327.68 | 83.46 | 95.69 | 110.74 |
| | **Std Dev.** | 2.34 | 3.09 | 3.21 | 4.24 | 4.85 |
| **Total** | **Maximum** | 325.92 | 342.09 | 110.54 | 117.61 | 163.00 |
| | **Mean** | 311.16 | 326.58 | 99.25 | 105.38 | 137.86 |
| | **Minimum** | 301.41 | 311.30 | 83.46 | 90.40 | 110.74 |
| | **Std Dev.** | 5.74 | 5.54 | 7.17 | 6.34 | 11.68 |

Table 2 The Frequency of yearly maximum ice thickness from November to April. The row represents different year in cold season and the column represents yearly maximum ice thickness with the unit of cm.

| MIT / Month | <50 | 50-75 | 76-100 | 101-125 | 125-150 |
|---|---|---|---|---|---|
| **December** | 4 | 1 | 0 | 1 | 0 |
| **January** | 4 | 4 | 1 | 0 | 0 |
| **February** | 4 | 25 | 26 | 3 | 1 |
| **March** | 1 | 3 | 24 | 8 | 4 |
| **April** | 0 | 2 | 1 | 0 | 0 |
| **After April** | 0 | 3 | 0 | 0 | 0 |
| Total | 13 | 38 | 52 | 12 | 5 |

Table 3 Correlation coefficient between maximum ice thickness (MIT) and average snow depth (ASD), and air temperature on bank (BAT) with a dataset size of 120 stations. The asterisk indicates the significant level of correlation coefficients, ** means significant at 99% level ($p<0.01$), and * means
535 significant at 95% level ($p<0.05$).

| Correlation Coefficients | November | December | January | February | March |
|---|---|---|---|---|---|
| MIT vs. ASD | 0.17 | 0.66* | 0.53* | 0.59* | 0.75** |
| MIT vs. BAT | -0.90** | -0.80** | -0.55* | -0.30 | -0.45 |

**Figures**

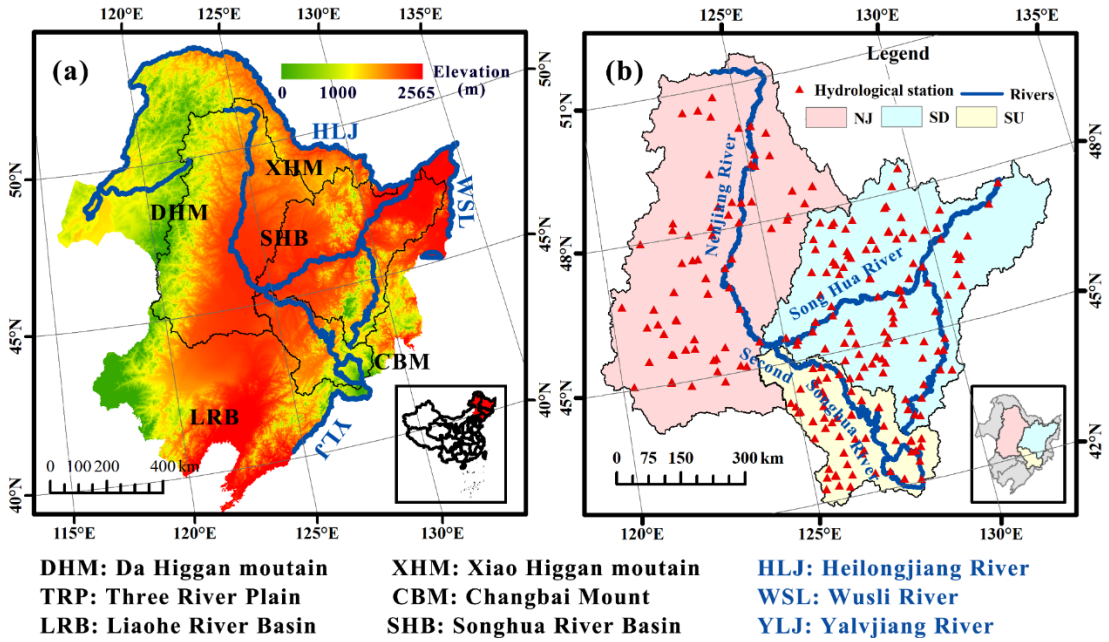


Figure 1 The geographic location of the Songhua River Basin showing (a) the elevation and (b) the location of 158 hydrological stations. The Songhua River Basin includes three sub-basins: Nenjiang River Basin (NJ), downstream Songhua River Basin (SD) and upstream Songhua River Basin (SU). Elevation data are from the Shuttle Radar Topography Mission (SRTM) with spatial resolution of 90 meters.

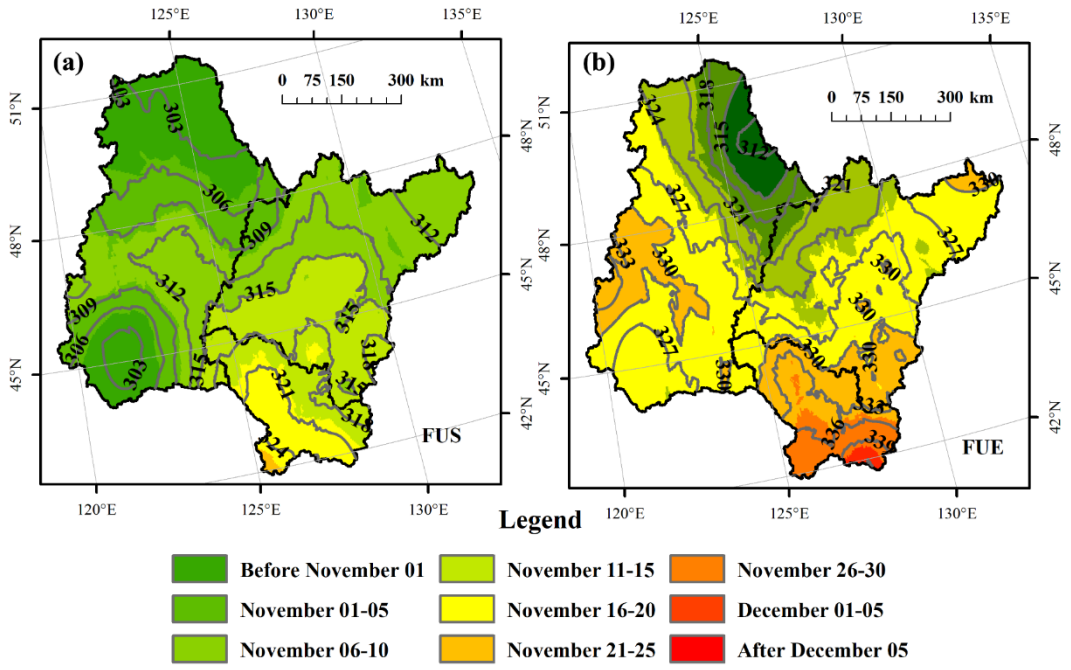


Figure 2 The average spatial distribution of freeze-up start (FUS) (a) and freeze-up end (FUE) (b) in the Songhua River Basin of Northeast China from 2010 to 2015. The number labels indicate the day of year (DOY) of the isophenes.

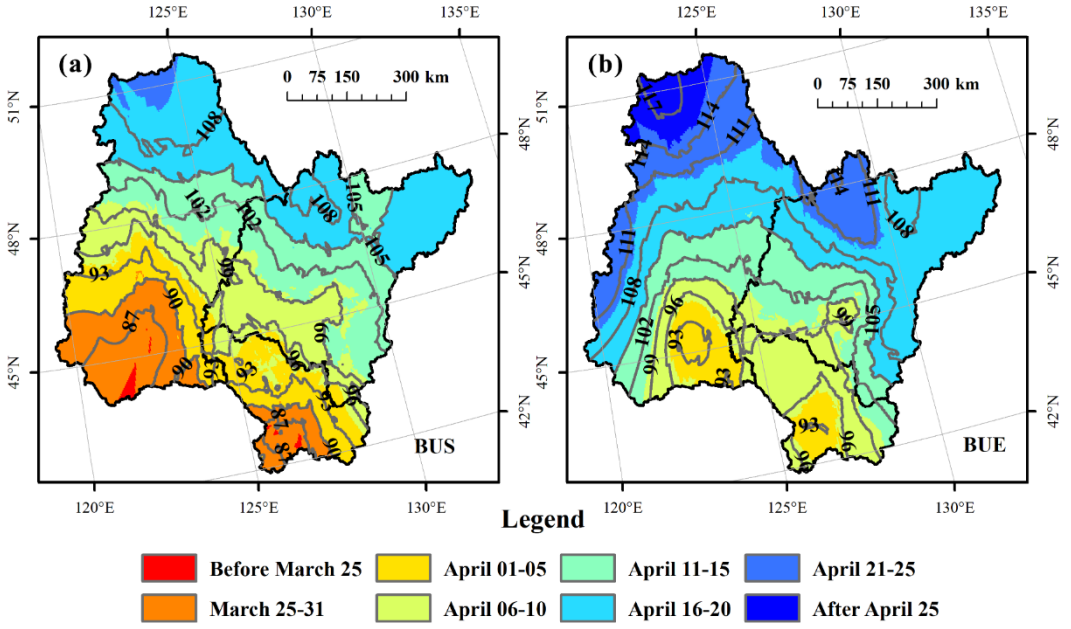


Figure 3 The average spatial distribution of break-up start (BUS) (a) and break-up end (BUE) (b) in the Songhua River Basin of Northeast China from 2010 to 2015. The number labels indicate the day of year (DOY) of the isophenes.

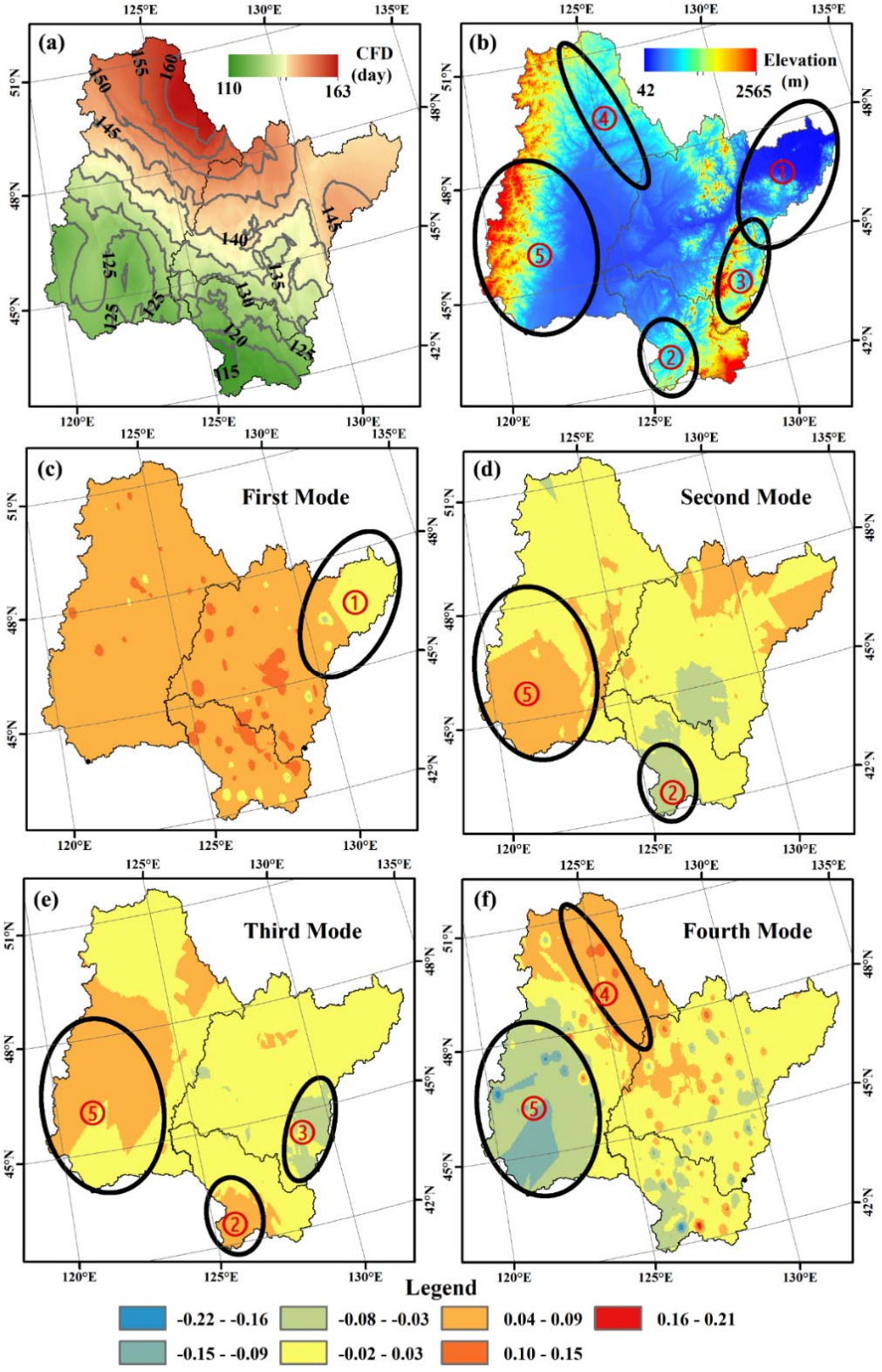


555

Figure 4 The spatial distribution of complete frozen duration (CFD) (a), five typical geographical zones (b), and first four principal components (c-f) decomposed by rotated empirical orthogonal function in the Songhua River Basin of Northeast China.

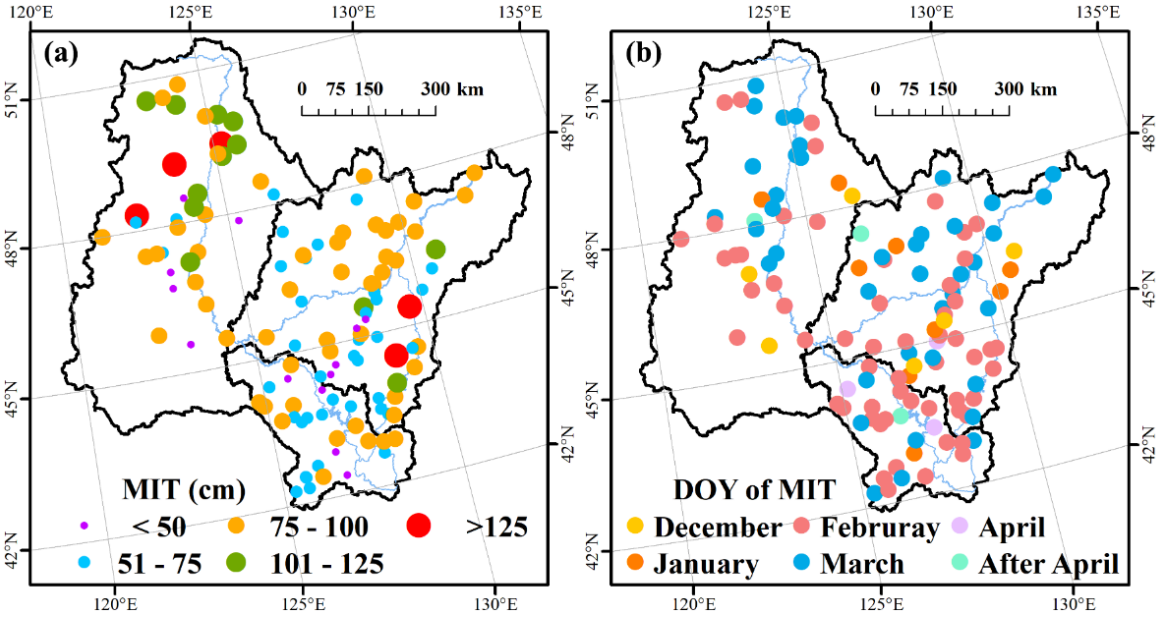


Figure 5 The spatial distribution of yearly maximum ice thickness (MIT) (a) of the river centre and the corresponding date (b).

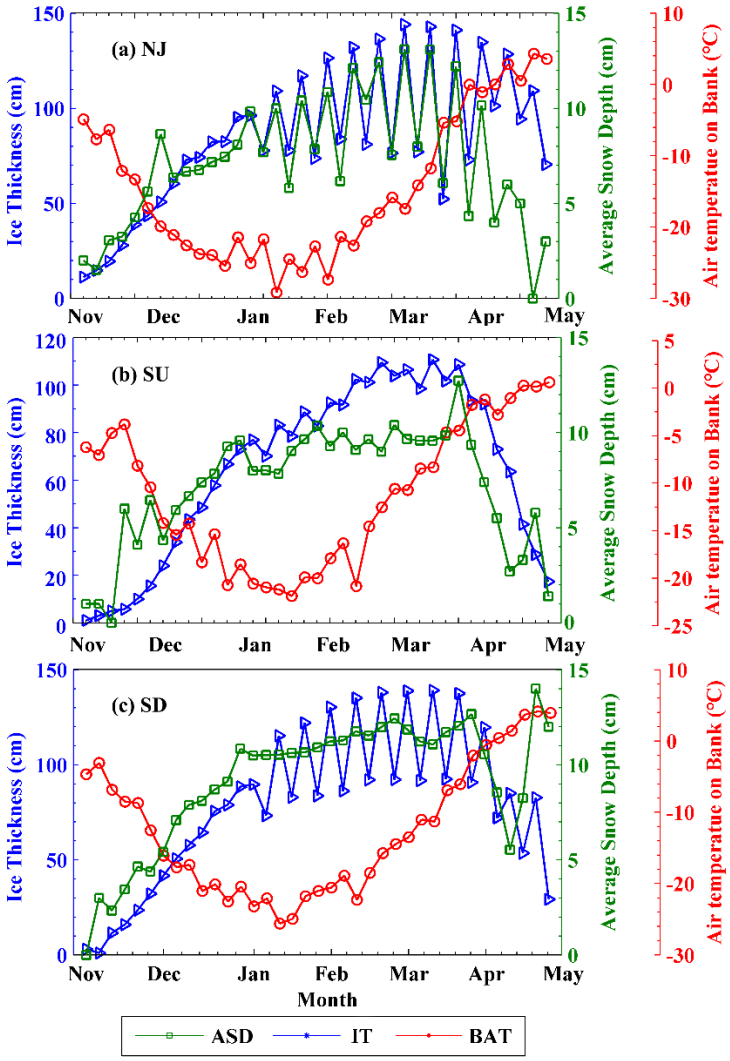


565 Figure 6 Average seasonal changes in ice thickness (IT), average snow depth (ASD) and air temperature on bank (BAT) from November to April for the period 2010 - 2015.

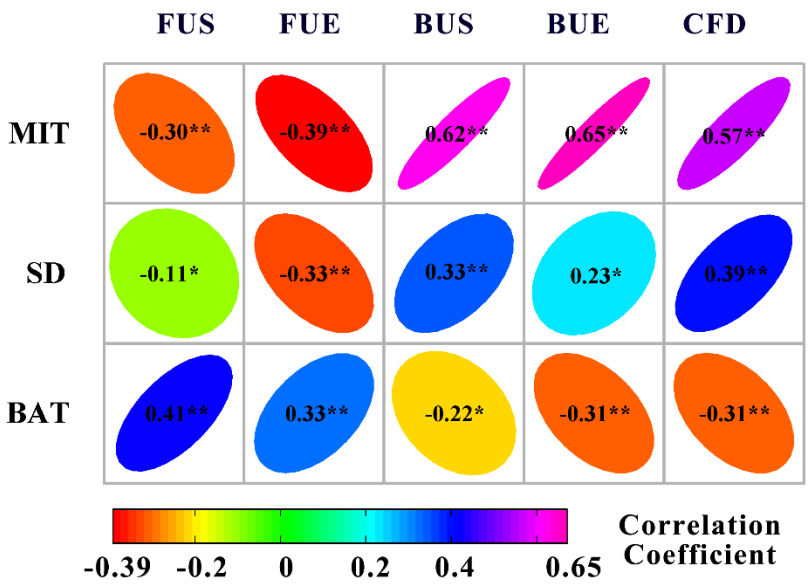


Figure 7 Correlation matrix between maximum ice thickness (MIT), average snow depth (ASD) and air temperature on bank (BAT) and lake ice phenology events with data from 120 stations. The asterisk indicates the significance level of the correlation coefficients, ** means significant at 99% level ($p<0.01$), and * means significant at 95% level ($p<0.05$).

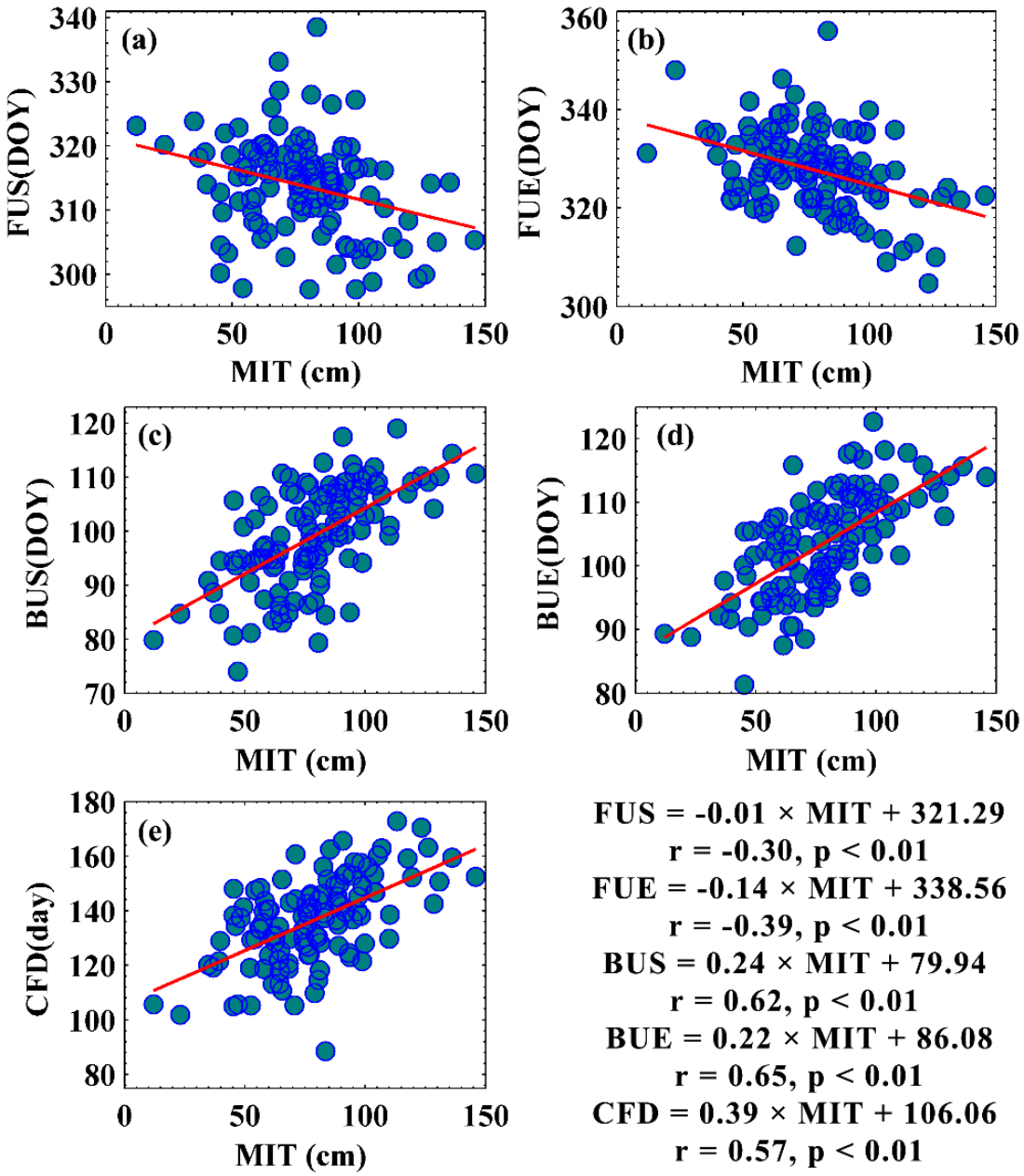


Figure 8 The bivariate scatter plots with linear regression lines between yearly maximum ice thickness (MIT) and ice phenology with dataset size of 120; r and p denote the correlation coefficient and p value of the regression line. The ice phenology events include freeze-up start (FUS), freeze-up end (FUE), break-up start (BUS), break-up end (BUE) and complete frozen duration (CFD).

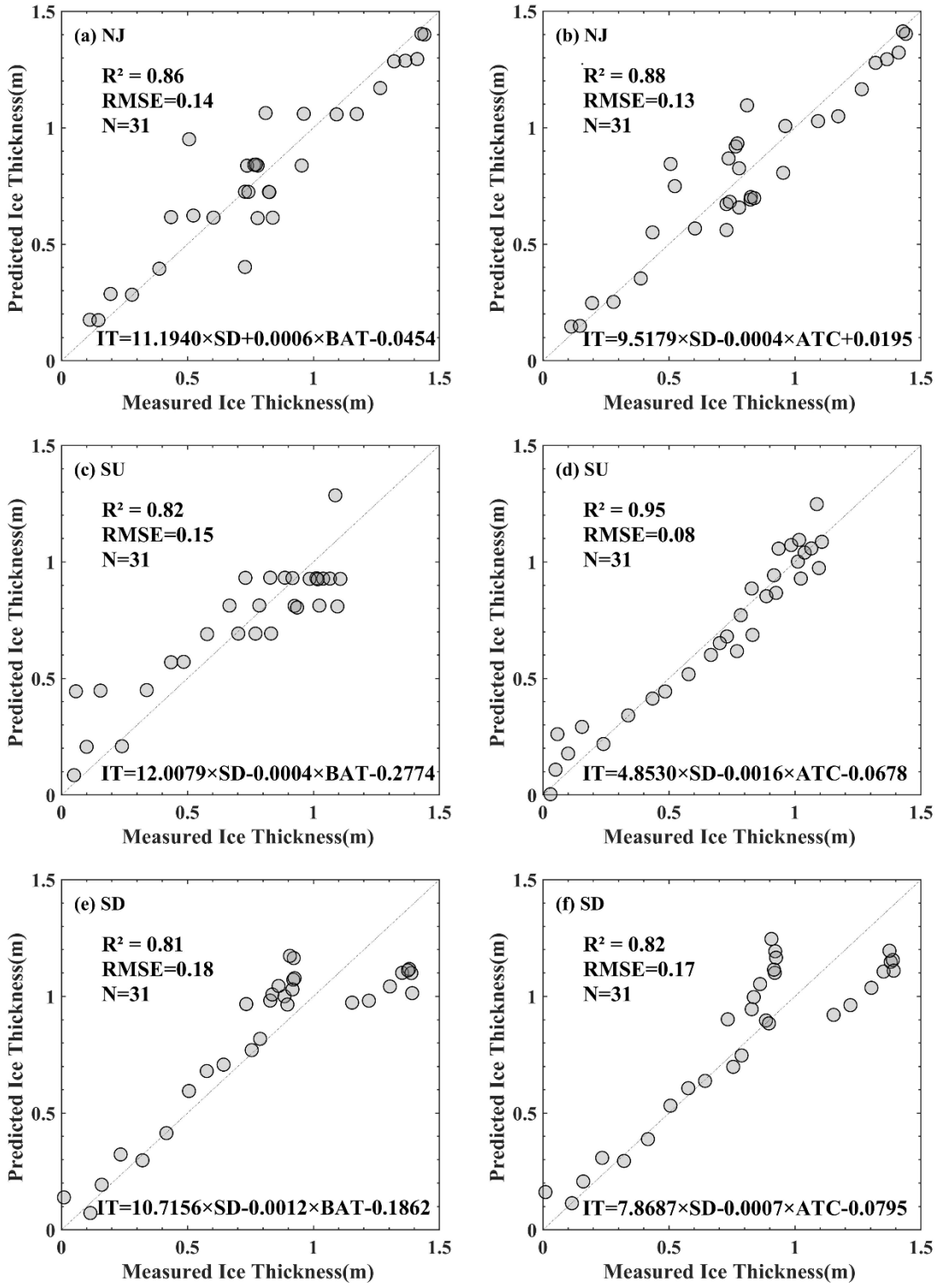


585 Figure 9 Scatter plots between measured and predicted ice thickness using Bayesian linear regression in three sub-basins (NJ: Nenjiang Basin, SU: upstream Songhua River Basin, and SD: downstream Songhua River Basin) in Northeast China. The model treated ice thickness as the independent variable, and snow depth and air temperature as dependent variables. Two types of air temperature were used: BAT represents air temperature on bank; ATC represents negative cumulative air temperature.